# Embedding Spatio-temporal Information into Maps by Route-Zooming

Guodao Sun, Ronghua Liang, *Member, IEEE,*
Huamin Qu, *Member, IEEE,* and Yingcai Wu, *Member, IEEE*

**Abstract**—Analysis and exploration of spatio-temporal data such as traffic flow and vehicle trajectories have become important in urban planning and management. In this paper, we present a novel visualization technique called route-zooming that can embed spatio-temporal information into a map seamlessly for occlusion-free visualization of both spatial and temporal data. The proposed technique can broaden a selected route in a map by deforming the overall road network. We formulate the problem of route-zooming as a nonlinear least squares optimization problem by defining an energy function that ensures the route is broadened successfully on demand while the distortion caused to the road network is minimized. The spatio-temporal information can then be embedded into the route to reveal both spatial and temporal patterns without occluding the spatial context information. The route-zooming technique is applied in two instantiations including an interactive metro map for city tourism and illustrative maps to highlight information on the broadened roads to prove its applicability. We demonstrate the usability of our spatio-temporal visualization approach with case studies on real traffic flow data. We also study various design choices in our method, including the encoding of the time direction and choices of temporal display, and conduct a comprehensive user study to validate our embedded visualization design.

**Index Terms**—Spatio-temporal visualization, occlusion-free visualization, least-square optimization

## 1 Introduction

The rapid development and deployment of various sensors such GPS devices in taxis in urban cities have been producing an increasing amount of spatio-temporal data. These data usually exhibit spatio-temporal patterns that are valuable for decision making and problem solving in urban transportation, planning, and management [29]. However, given the growing amount and complexity of the data, finding meaningful patterns and gaining insights from the spatio-temporal data have been challenging. Proper visualizations of the spatio-temporal data are an important means for uncovering such hidden patterns [8][23][27].

In recent years, a number of studies have been conducted to visualize and analyze spatio-temporal data. In general, proposed methods could be characterized into two basic categories, namely, *linked views* and *integrated views*. In linked views, map that visualizes spatial attributes of data is placed into one window, and other related information (e.g., temporal displays) into other windows. However, users may experience memory context switching burden when linking these views to discover possible correlations [28]. Thus, placing spatio-temporal information near the spatial context is desirable so that users can easily link related information with its spatial context.

- *Guodao Sun and Ronghua Liang are with Zhejiang University of Technology. Ronghua Liang is the corresponding author. E-mail: godoor.sun@gmail.com, rhliang@zjut.edu.cn*
- *Huamin Qu is with Hong Kong University of Science and Technology. E-mail: huamin@cse.ust.hk*
- *Yingcai Wu is with State Key Lab of CAD & CG, Zhejiang University. E-mail: ycwu@zju.edu.cn*

In integrated views, maps and spatio-temporal information are integrated into one display to facilitate the discovery of spatio-temporal patterns. To create integrated views, a straightforward way is to stack the information onto the map directly or in the form of 3D, however, it would cause occlusion and visual clutter.

Given that many spatio-temporal information (such as vehicle trajectories and roadside air pollution levels) are often related to roads, it will be desirable to put those information onto the roads in a map for "in-place" occlusion-free visualization of spatio-temporal patterns while preserving the spatial context. Nevertheless, this process is a daunting challenge because of three major obstacles that should be overcome. First, in order to clearly perceive the information that embedded on narrow roads on a map, the map must be zoomed into a very high. Although the most natural way is to zoom linearly, linear zooming will push much of the spatial context out of the display area. Thus, one need to explore a non-linear zooming method that broadens the roads of interest while preserving the spatial context as well as users' mental map. Second, if only temporal displays are embedded into roads, encoding the flow direction of time on a road remains unclear since roads are always of arbitrary direction and temporal displays often involve a time axis. Third, the temporal displays which are suitable for embedding into roads remain unclear.

To address these issues, we present a novel context-preserving visualization technique called route-zooming to seamlessly integrate spatio-temporal information maps for occlusion-free analysis of spatio-temporal data. This method automatically broadens a specified route to display temporal visualizations, thereby allowing in-place,

occlusion-free visualization of spatio-temporal data. We transform the problem of route-zooming to a non-linear least squares optimization problem by defining a proper energy function, which guarantees the selected route is broadened on demand with least distortion to the map.

Embedding temporal displays on roads raises the question on how to indicate the direction of time flow. We investigate different choices of encoding time direction since a conventional time direction that always points from left to right or from bottom to top is not applicable. We further evaluate the usability of our design based on a controlled user study against a traditional linked view method. Our approach is general and we discuss different kinds of temporal displays which are suitable for being overlaid on roads in a map. To the best of our knowledge, this paper is the first comprehensive study on embedding temporal displays into roads in a map. We demonstrate the usefulness and usage of our spatio-temporal visualization with two case studies on real taxi trajectory data.

In our previous work [22], we used an image-based seam carving technique to broaden a route. However, this technique has a severe limitation wherein the roads nearby may also be broadened to various degrees when broadening a route. This situation is significantly noticeable when the routes are usually wiggly or even form a loop. In addition, the technique is slow and cannot enable interactive user experience. In this work, we replace the image-based technique with a novel, robust network deformation technique that could broaden any kind of route effectively and efficiently. Furthermore, we introduce two additional application instantiations including an interactive metro map and a visualization of traffic simulation to demonstrate the applicability and usefulness of the new technique. Moreover, we use two compressive case studies to show the effectiveness of our in-place visualization method for spatio-temporal data analysis. The major contributions of our work are as follows:

- A novel route-zooming technique that successfully broadens any route with least distortion to the map.
- An intuitive visualization that allows in-place, occlusion-free exploration of spatio-temporal patterns with preserved spatial context.
- A systematic study of the key design choices such as encoding of time direction and a quantitative and qualitative evaluation of the in-place visualization.

## 2 Related Work

### 2.1 Non-Linear Zooming

This section reviews and discusses focus+context (mainly non-linear zooming) techniques in visualization and computer graphics. The comparison of our method with linear zooming can be found in Section 4.5. Focus+context is a widely used approach to show the focus and context content simultaneously in a single display. Many focus+context techniques and systems, such as fisheye view [9], SignalLens [14], point-based map distortion [6], TreeJuxtaposer [17], LiveRAC [16] , Chronolenses [30], and Sigma Lenses [19] have been developed to visualize data from different problem domains. A handful of recent works also applied focus+context to maps [11]. Although these techniques achieve the integration of focus regions into surrounding context, they often introduce undesired distortions that make them unsuitable for our analytical tasks. Seam carving [5] is a popular image resizing technique that enlarges or shrinks an image with minimum distortion. Qu et al. [20] used a seam carving technique to broaden a selected route to increase its visibility in a 3D city environment. Our previous work [22] adopted a similar strategy to broaden routes to overlay temporal displays. In seam carving a seam is inserted into an image either horizontally or vertically, and thus the seam length is always equal to the width or height of the image. Thus, when broadening a curved or zigzag road, a number of seams have to be inserted in not only the road of interest, but may also other adjacent roads (see Figure 5). Another limitation of the algorithm is its poor time performance, which prevents interactive exploration and visualization.

Graph-based deformation techniques [11], [25], [26] deform the road network of a map directly to offer more flexible focus+context visualization. Haunert et al. [11] enlarged a focus region in a map with the overall road network bounded inside a box. Thomas et al. [25] proposed an efficient algorithm based on [11] to enable a user to interactively enlarge a focus region in a map. Wang et al. [26] presented a focus+context metro map, where metro stations are repositioned to highlight a focus route. However, these techniques only focus on the translation of a selected route [26] or zooming of a selected region [11], [25] without changing the size of the roads inside the region. These techniques cannot be used to broaden a route (route-zooming) for information overlay with least distortion to the overall road network. In this work, we deform the road network of a map directly to allow efficient and robust route-zooming.

### 2.2 Spatio-Temporal Data

A recent survey by Andrienko et al. [3] raised the need of finding effective visualizations of temporal dimension in geospatial data. The existing work could be roughly divided into two categories, namely, linked views, where the spatial and temporal aspects of data are displayed in coordinated multiple views, and integrated views, where the temporal information is displayed with geospatial visualization in the same view.

**Linked View** Linked-view methods have become standard approaches to display temporal and spatial data [3]. Ivanov et al. [12] used several synchronized views, including a timeline, a map, and a camera view, for efficient monitoring of spatio-temporal data collected through surveillance cameras. Andrienko et al. [4] combined a time graph with a map to visualize multiple trajectories. Guo et al. [10] presented a trajectory analytics system with a map view for spatial data and a stacked graph along with a scatter plot for temporal data. Although multiple coordinated views is a powerful visualization technique, a

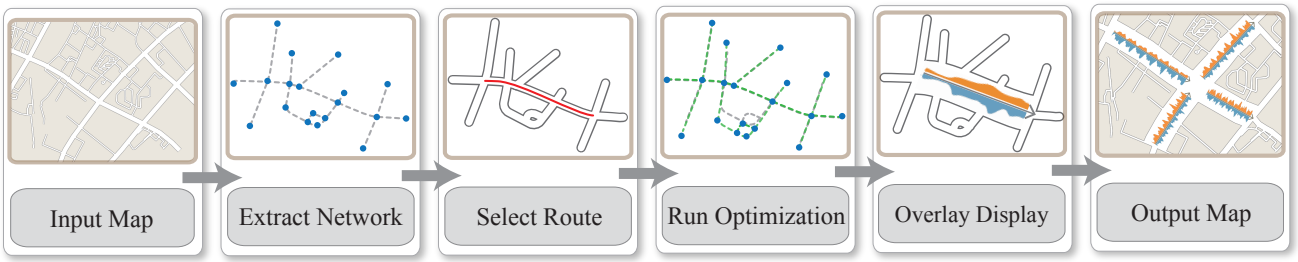


Fig. 1: Our system pipeline for creating an in-place, occlusion-free visualization of spatio-temporal data.

significant limitation of such methods is the cost of screen real estate to show views side-by-side.

**Integrated View** A well-known technique in geographic applications that integrates space and time in the same view is the famous space-time cube [13]. The 3D space-time cube presents space as a 2D map and time as the third dimension. However, this approach does not scale well to a large number of samples because of the occlusion problem in 3D space. Tominski et al. [24] proposed a so-called 2D/3D hybrid display to stack trajectories as bands in the third dimension, whereas time is integrated by appropriate ordering of trajectory bands. However, the view will be severely hindered if one wants to visualize trajectories on multiple roads simultaneously. Liu et al. [15] displayed a circular time axis enclosing a road map to encode both temporal information about trajectories and spatial context. However, the design is limited in the number of roads that can be viewed and only works for cyclical time. Methods that directly embed time series curves on top of their spatial locations in two dimensional maps, such as the embedding of ThemeRiver in a map [1], lead to severe occlusion of other useful map information and visual clutter. Abstraction and aggregation methods could also serve the purpose of integrating space and time. Crnovrsanin et al. [7] proposed proximity PCA to transform spatial information into abstract space and plot proximity spatial information against the time axis. Andrienko et al. [2] discussed possible aggregation methods of movement data. Scheepens et al. [21] presented a density map of traffic data, using color to represent time.

In contrast to the above approaches, our method aims to totally avoid the occlusion problem. It relies on a novel non-linear zooming algorithm to broaden the roads without distorting other areas too much and then overlays temporal displays onto the roads.

## 3 System Overview

Figure 1 shows the pipeline of our system to create an in-place, occlusion-free visualization of spatio-temporal data. The input map is in GeoJSON format, a widely used format for encoding geographic data structures. We use Java OpenStreetMap Editor to generate the input for our system. The input map is then transformed into a road network represented by a graph data structure. Users can select a route, followed by a road network optimization process that broadens the route with least distortion to the other parts of the road network. Finally, various displays could be overlaid onto the broadened route.

Road network optimization and display overlay are two core parts of the system. In the first part, the route-zooming problem is transformed into a nonlinear least squares optimization problem through an energy function based on a set of well-defined optimization constraints. Our system solves the optimization problem efficiently in a linear least squares sense. In the second part, users could interact with the system to overlay various information, such as time series curves, onto the broadened route. This process helps create a focus+context visualization with seamless integration of spatial and temporal data to facilitate various spatio-temporal data analytics tasks.

Our system is designed to support various types of tasks that are commonly performed in spatio-temporal analysis:

**T1. Level-of-Detail Characterization** Identify the trends and variations of attributes over different time periods in a large or local area.

**T2. Pattern Detection** Locate a specific pattern of attributes in its occurring spatial and temporal positions.

**T3. Pattern Comparison** Compare the patterns of attribute values across different time intervals and different spatial regions.

## 4 Road Broadening Algorithm

In this section, we first describe the limitations of the existing methods for broadening roads, discuss the advantages of our graph-based method, and define the problem of route-zooming as an optimization problem. We then introduce an energy function used for the optimization and present the solution to solve the problem. We finally test our method against the seam carving and linear zooming methods.

### 4.1 Problem Definition

The existing seam carving based methods [20], [22] have limitations. First, when broadening complex roads (denoted by focus roads), such as curved or zigzag roads, seams are inserted in the roads and other maps either horizontally or vertically. As a result, the context roads or other regions near the focus roads are likely to be distorted to various sizes (see the two results in the middle column of Figure 5). Thus, the resulting map is often distorted to a large extent, which can mislead users. Second, seam carving performs poorly in route-zooming in a large map. The algorithm needs to calculate an optimal seam to be inserted into the map iteratively for many times to resize the route, which is a time-consuming process.

To overcome the problems of existing methods, we propose a graph-based method to support effective and efficient route zooming. Our method accepts a GeoJSON map as the input data, which could be represented by a graph with a set of nodes and edges. The method allows direct manipulation of the graph, which provides much flexibility to handle complex roads effectively. We define an energy function in a non-linear least squares form that guides manipulation in the following optimization process. Our well-defined energy function ensures that the selected route is broadened successfully whereas the distortion to the whole graph is minimized. Moreover, the optimization problem could be solved in one single step, which improves performance significantly.

To broaden a route by optimization, our main idea is to introduce a constraint to add more drawing space for the focus roads, and a constraint to minimize the distortion to the context roads. We also minimize the bending of all the roads because bending roads could lead to undesired, irregular results, particularly for metro maps. In addition, the map should stay in a bounding box and each node should be close to its original position as much as possible to preserve user's mental map. We formulate the constraints into different optimization energy terms, namely, energy terms with respect to *focus road deformation*, *context road deformation*, *road bending*, and *node translation*. The energy terms are finally assembled into an energy function. Therefore, the problem of route-zooming is transformed to an optimization problem. The goal of the optimization is to find the new position of each node in the road network with the energy function minimized.

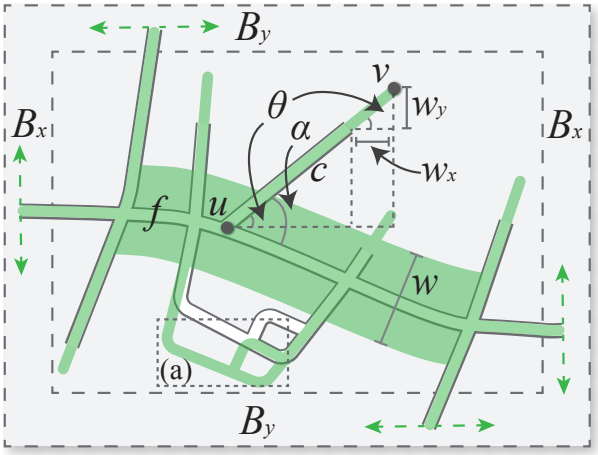


Fig. 2: Illustration of the optimization algorithm for route-zooming. The original road network is outlined in gray contours, whereas the optimized network is denoted by solid green areas. We denote a focus road by $f$ (to be broadened by width $w$), a context road by $c = \{u, v\}$, the bounding box constraint by $B_x$ and $B_y$, the angle of incline of the context road by $\theta$, and the angle between the focus road and the context road by $\alpha$.

### 4.2 Energy Function for Optimization

A map is often crisscrossed by roads with different styles, which essentially forms a road network. The road network could be formally represented by a connected graph $G = (V, E)$ to preserve its topology, where $V$ is the set of nodes (road junctions) and $E$ is the set of edges (road segments). Node $u \in V$ has a geospatial position $(x_u, y_u)$ and edge $e \in E$ is denoted by $\{u, v\}$ where $u, v \in V$. When a route is broadened to a certain width, each node $u$ of the road network will have a new position $x_u'$ and $y_u'$. For simplicity, we indicate the roads to be broadened by *focus roads*, and the others by *context roads*. We denote the set of nodes on the focus roads by $V_F$, and the set of neighboring nodes connected to node $u$ by $V_{N(u)}$. We detail the definition of each energy term and the energy function as follows.

**Focus Road Deformation** To retain sufficient space for the broadened focus roads, the context roads connecting the focus roads must be shifted outward a certain distance (See Figure 2). Thus, if a focus road $f$ is broadened to have a width of $w$ (see the large green road in Figure 2), the nodes on the context roads connecting the focus roads are moved away by $w_x$ and $w_y$ in the horizontal and vertical directions, respectively. From Figure 2, it is easy to compute that $w_x = \frac{w}{2sin(\alpha)} cos(\theta)$ and $w_y = \frac{w}{2sin(\alpha)} sin(\theta)$ where $\alpha$ indicates the angle between the focus road and the context road, and $\theta$ represents the angle of incline of the context road. To broaden the focus road, we define the energy term:

$$\begin{aligned} &\forall u \in V_F, v \in V_{N(u)}, v \notin V_F : \\ &\quad D_{Focus} = |(x_u' - x_v') - (x_u - x_v) - w_x|^2 \\ &\qquad + |(y_u' - y_v') - (y_u - y_v) - w_y|^2 \end{aligned} \tag{1}$$

where node $u$ represents the conjunction of focus road $f$ and context road $c$, and node $v$ is the node on the other side of road $c$. The equation has deformation terms for both $x$ and $y$ components of the two nodes. Obviously, if $D_{Focus}$ is minimized to 0, then the horizontal and vertical distances between $u$ and $v$ are extended by $w_x$ and $w_y$. When applying to multiple roads, the algorithm will iterate each of the focus roads, and create corresponding energy terms.

**Context Road Deformation** To preserve the original overall structure of the road network, context roads should not be scaled. Thus, we define the following deformation energy term for the context roads:

$$\begin{aligned} &\forall u \notin V_F, v \in V_{N(u)}, v \notin V_F : \\ &\quad D_{Context} = \frac{1}{Dist(u,v)} (|(x_u' - x_v') - (x_u - x_v)|^2 \\ &\qquad + |(y_u' - y_v') - (y_u - y_v)|^2) \end{aligned} \tag{2}$$

This energy term aims to ensure that context road $c = \{u, v\}$ could be translated because of the deformation of focus roads, but it should not be scaled (see the context roads in Figure 2 (a)). $Dist(u, v)$ is the Euclidean distance between node $u$ and $v$. By multiplying $1/Dist(u, v)$, longer roads are less sensitive to the scaling and could be slightly scaled.

**Road Bending** In addition to the constraints for focus and context road deformation, we impose another important

constraint on road bending. This constraint is particularly useful when a road network (such as the road map of Lower Manhattan in New York) has a regular, grid-style structure. The deformed road network should still preserve the regular grid-style shape, which could be achieved using the following energy term:

$$\forall u,v \in V : D_{Bending} = |atan2(y_u^{'} - y_v^{'}, x_u^{'} - x_v^{'}) - atan2(y_u - y_v, x_u - x_v)|^2 \quad (3)$$

The energy term helps preserve the angle of incline ($\theta$) of the context road $c = \{u,v\}$ after optimization. This energy term is important, especially our method is applied to metro maps because many of them adopt an octilinear layout to draw metro lines. Therefore, to obtain a deformed but still octilinear metro map, it is necessary to impose such constraint and even increase the weight of the energy term.

**Node Translation** To preserve the extent of the road network, all nodes should be within a bounding box. Following [25], we define two energy terms:

$$\begin{aligned} \forall u \in B_x : \quad & D_{Bx} = |x_u^{'} - x_u|^2 \\ \forall u \in B_y : \quad & D_{By} = |y_u^{'} - y_u|^2 \end{aligned} \quad (4)$$

where $B_x$ and $B_y$ represent the areas adjacent to the boundary of the map within a certain distance. The distance cutoff is set to 10% of the side length of the bounding box after some experiments to create appropriate deformed results. Every term constrains the nodes in the $B_x$ (or $B_y$) area to be moved only in the vertical direction (or horizontal direction); thus the nodes in areas $B_x$ and $B_y$ do not move out of the bounding box (see Figure 2).

To preserve users' mental map after optimization, we hope the roads, particularly the focus roads, should be close to their original positions as much as possible. Thus, we introduce the following energy term:

$$\forall u,v \in V_F : D_{Preferred} = |x_u^{'} - x_u|^2 + |y_u^{'} - y_u|^2 \quad (5)$$

The energy term imposes a constraint that the nodes on the focus roads should not be moved far away. The constraints of focus roads deformation and context roads deformation could propagate through the entire road network and help preserve the positions of the nodes on context roads.

We define an energy function using a weighted summation of the aforementioned energy terms to obtain a desired new road network:

$$D = \omega_f D_{Focus} + \omega_c D_{Context} + \omega_s D_{Bending} + \omega_b D_{Bx} + \omega_b D_{By} + \omega_p D_{Preferred} \quad (6)$$

### 4.3 Road Network Optimization

The energy function defined in Equation (6) is in an obvious non-linear least squares form that can be solved by a typical linear least squares solution. The energy function is an overdetermined system, and matrix $A$ and vector $b$ could be constructed in a linear least squares form (namely, $Ax = b$). The number of the columns and rows in $A$ correspond to the number of variables and constraints, respectively. $b$ is a single column vector where the number of rows is equal to the number of constraints. The solution, namely, the output position ($x_u^{'}$, $y_u^{'}$) of the nodes in the optimized map, could be obtained with the following equation.

$$\hat{\beta} = (A^T A)^{-1} A^T b \quad (7)$$

where vector $\hat{\beta}$ stores $x_u^{'}$ and $y_u^{'}$. All the constraints imposed are soft constraints; hence, they may be violated to certain degree. Nevertheless, this problem could be handled with carefully specified weights. $\omega_f$ is used to ensure that the focus road is broadened to a specified width. When many roads connect to a long focus road, users could increase $\omega_f$ to ensure the road broadening effect. $\omega_c$ is used to ensure that the deformed road network still preserve the overall structure of the original one. When a road map exists many dense context roads, one could increase $\omega_c$ to avoid the intersection among the deformed context roads. $\omega_s$ is particularly useful for ensuring the regular structure of the road network. For example, when operating with a metro map, $\omega_s$ could be set higher to keep the octilinear structure of the metro map. $\omega_b$ is used to ensure that the deformed maps still preeserve the extent of the road ntwork, and we always set it to a higher value (e.g., 10). $\omega_p$ is preventative parameter and used to ensure the deformed focused roads still hold their original positions approximatively. In our experiments of general maps, we set $\omega_f = 1$ , $\omega_c = 1$, $\omega_s = 0.5$, $\omega_b = 10$, and $\omega_p = 0.1$.

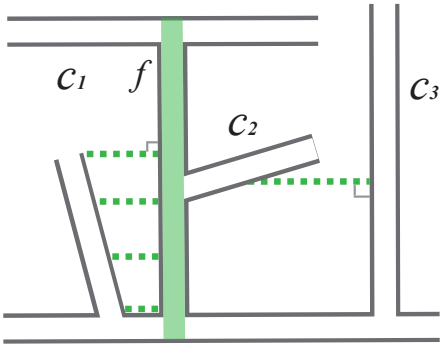


Fig. 3: Illustration of the process for handling road intersections when broadening a road. The focus road to be broadened is highlighted in green, and the virtual roads added are represented by dash line segments

### 4.4 Techinques for handling road intersection

When a focus road is being broadened to a relatively large width, it may intersect with nearby context roads. For example, in Figure 3, if focus road $f$ is being broadened continuously, it may finally intersect with context road $c_1$, or the displaced context road $c_2$ may intersect with context road $c_3$. This situation may lead to undesirable perceptual distortion or interference since the topology of the road network is different from the original one.

We address this problem by inserting *virtual roads* between the focus roads and the intersected context road. When the road broadening is finished, the algorithm will check whether the output road network introduces new road

intersection or not. If none of them is found, then the road broadening process is done. Otherwise, virtual roads (see the dashed green lines in Figure 3) will be inserted into the road network and the road broadening algorithm is performed again to obtain a crossing-free road network. Though inserting a mass of virtual roads will immediately relax this issue, the context roads (e.g., $c_1$ and $c_3$) will be moved away too much due to the impact by *Focus Road Deformation*, which may further introduce other road intersection. Using insufficient number of virtual roads may not guarantee a crossing-free result. Thus, we adopt an iterative strategy to insert virtual roads. The number of the inserted virtual roads begins initially with one. If the road broadening process with one virtual road relaxes the issue, then the algorithm is done. If not, the number of inserted virtual roads increases exponentially. The inserted virtual roads will be evenly distributed among intersection roads. In practice, we find that the road intersections are usually avoided by inserting two or four virtual roads. The pseudo-code of above process is given in Algorithm 1.

**Algorithm 1** Handling Road Intersection

**Input:** A deformed road network, $n = 0.5$
**Output:** A road network without road intersection
  **while** road intersection exists **do**
    $n = n * 2$
    insert $n$ *virtual roads*
    run *route-zooming* algorithm
  **end while**

### 4.5 Technique Comparison

In this section , we compare our method with a seam carving based method [20], [22]. In the two maps in the left column of Figure 5, we select two areas from the maps of Hong Kong and London, respectively. A zigzag road and a loop road (highlighted in red) are chosen to be broadened. The results processed by seam carving are shown in the middle column of the figure, whereas the results generated by our method are shown in the right column.

The seam carving based method could successfully broaden the focus roads while minimizing the distortion to the overall structure of the map. However, the context roads connected to the focus roads are also broadened to have various widths (middle column in Figure 5), which may become a serious issue when a user examines the deformed map and wants to distinguish the focus roads and context roads. With our method, only the selected roads are broadened to a desired width, and the context roads are not broadened so the distraction is avoided.

We further conduct two comparisons with different and complex maps including U.S. highway maps and a complex road junction (see Figure 4). When broadening a selected focus road, the seam carving based method will also broaden or distort context roads to different extent (middle column in Figure 4). In addition, when broadening a roundabout road using seam carving based method, the road will be divided into several road segments with horizontal or vertical direction. Thus, the focus road may be broadened excessively due to retargeting the remaining part of the map image. In some cases, the seams will bypass certain thin context roads, and may result in a map with salient visual difference. With our method, only the focus roads are broadened to a desired width, and structure of the context map is not affected.

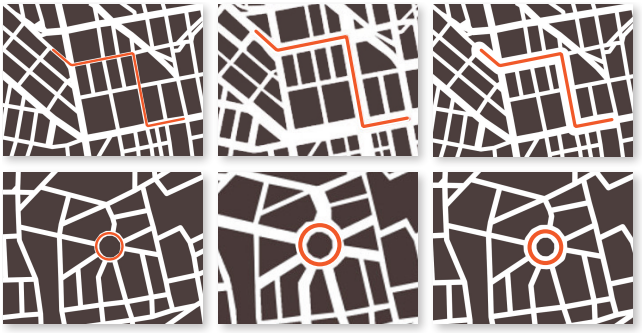

Fig. 5: Comparison of the route-zooming algorithm with the seam carving based method for broadening a focus route highlighted in red.

## 5 Visualization Design

After the roads are broadened by our route-zooming approach, we can now overlay various information onto the road. Overlaying spatial information is straightforward, one could broaden the road to an appropriate width, and directly put the information onto the place that is near to its geographical position. However, overlaying temporal information brings some critical challenges, including how to encode the time direction of the displays on the road, and the choices of visualization design. We aimed to address such issues as follows.

### 5.1 Time Direction

Embedding temporal displays on roads raises the question on how to indicate the direction of time flow. Given that the road on which the time series is overlaid could be of any slope, conventional default encoding where time flows from left to right does not apply. Figure 6 illustrates various design choices considered in our system.

**Default Direction** In principle, we can encode time direction based on the Cartesian coordinate system. The time flow direction will be from left to right for horizontal roads and from bottom to top for vertical roads. For roads with other slopes, we can choose a direction based on the angle between the road and the horizontal axis. For example, if the angle between the road and the horizontal axis falls between $-45$ degree to 45 degree, then the time direction is from left to right; otherwise, the direction is from bottom to top. Although intuitive and natural, the approach is problematic under special circumstances. For example, a road with a 43 degree slope may adopt a left-to-right orientation, whereas a road with a 47 degree slope will adopt a bottom-to-top orientation. Thus, slight changes in the slope can lead to a dramatic flip of time flow direction.

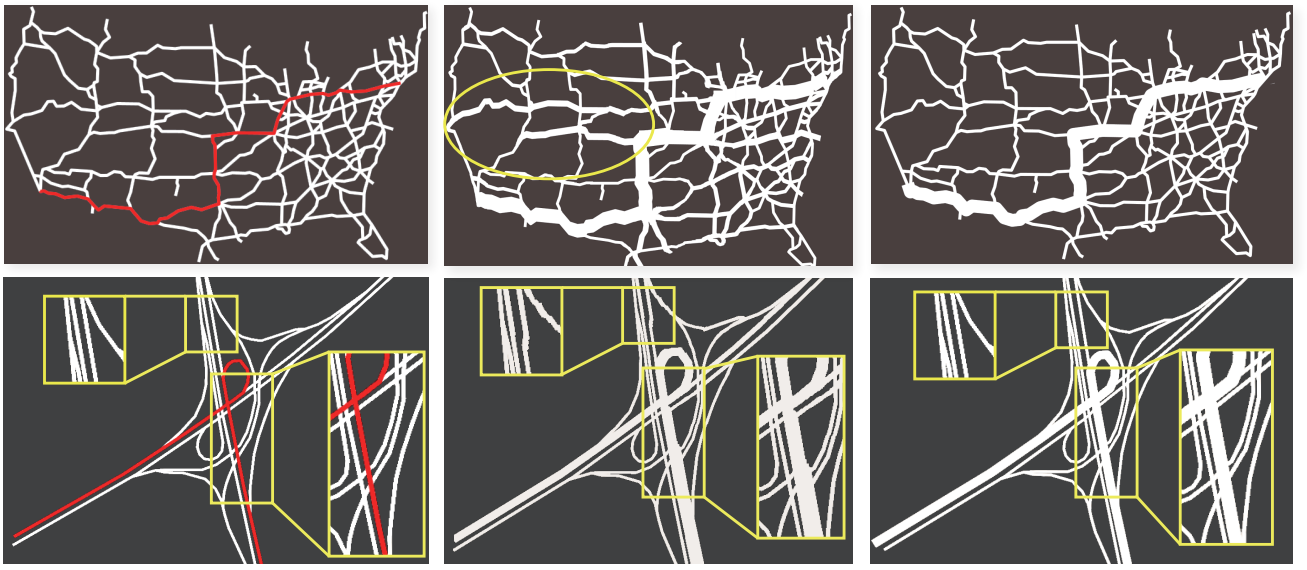

Fig. 4: Technique comparison with U.S. highway maps and a complex road junction.The focus routes are highlighted in red in the left two figures, the middle two figures are the results created by the seam carving based method, and the right two figures are the ones created by our route-zooming method.

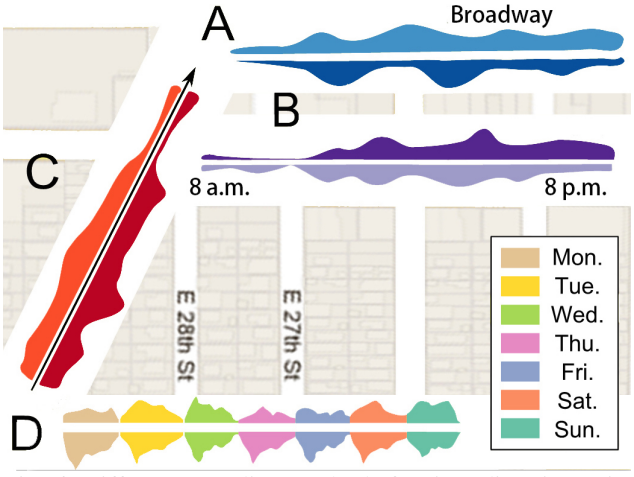


Fig. 6: Different encoding methods for time direction using road name (A), text labels (i.e.,date and time) (B), visual symbols (i.e., arrow) (C), and color (D).

**Possible Visual Cues** For special cases, additional visual cues (e.g., text labels, visual symbols, colors, and animations) are required to indicate time direction. With **text labels**, we can label the date and time directly alongside the temporal pattern, however, a trade-off will occur between the space taken up by the text and the legibility of the label. There also exists a handful of conventional **visual symbols** for encoding direction, for example, a time axis with an origin and arrow is the simplest, most non-pervasive, and most natural way to indicate direction. The **color** channel of the temporal design can be exploited using saturation, opacity, or a sequential color scheme to indicate time direction. **Animation** can be used to represent the flow orientation of time or to directly animate time-varying data.

**Relying on Existing Map Features** Assigning time direction according to the orientation of the text name label of the road presents two obvious advantages. First, our design principle of minimal occlusion or distortion is satisfied because the design relies on existing map features. Second, from the perspective of users, associating street names orientation with time direction is simple to learn and easy to apply.

Table 1 summarizes and compares different schemes for encoding time direction on a road. All schemes have their advantages and disadvantages. Determining which one to use depends on its application, the familiarity of users with our system, and the space capital available for visualization. In previous work [22], we conducted an user study to compare the performance of two time direction encodings, i.e., *Visual Symbol* and *Relying on Existing Map Features*, and found that using additional visual symbol slightly outperforms the one that only relies on existing map features, and the response accuracy between them are comparable.

| Name | Extra Space | Ambiguity | Accuracy |
|---|---|---|---|
| Default | No | Yes | Medium |
| Text Label | Yes | No | High |
| Visual Symbol | Yes | No | High |
| Color | Yes | Yes | Medium |
| Animation | No | No | Medium |
| Road Name | No | Yes | High |

TABLE 1: Different schemes for encoding time direction.

### 5.2 Temporal Display

Another design choice is to decide which temporal displays are suitable for being overlaid on roads in a map. There is one road characteristic that cannot be changed by broadening: long but narrow. The ratio and limited width are the major constraints for our design choices. First, line charts and its variations (e.g., horizon graph) should have no problem with our scheme. Second, Themeriver can also be used. However, we must ensure that the road is adequately broadened so that each layer is visible to

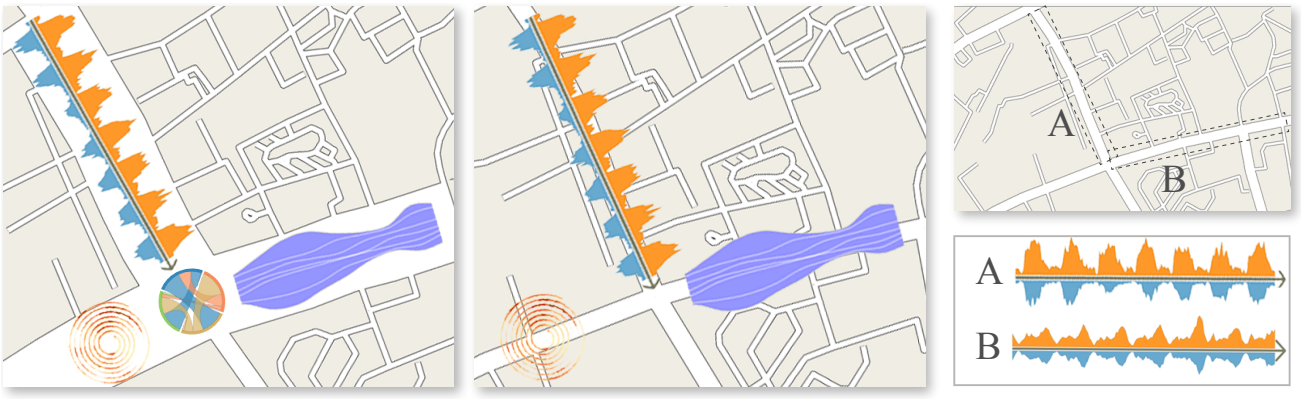


(a) (b) (c)

Fig. 7: A comparison of three views for spatio-temporal data visualization, namely, embedded view, integrated view, and linked view: (a) various temporal displays are overlaid on the broadened roads to achieve occlusion-free visualization; (b) temporal displays on the original, undeformed roads occlude important neighboring context; and (c) temporal displays in separate views lead to a considerable burden of context switching.

users. Third, the visualization of cyclical temporal patterns (e.g., radial views) can be overlaid on the road but is not easily recognized unless the road is broadened to a huge width. However, the radial view (e.g., chord diagram) is suitable for presenting the interchange of traffic flow in the intersections of multiple roads. We demonstrate these embedded temporal displays in Figure 7 (a).

Figure 7 (b) and (c) present a comparison of our embedded view with two other views (i.e., integrated view and linked view), respectively. The integrated view cannot avoid the occlusion problem because the temporal displays are always directly overlaid onto the original roads. The linked view requires users to mentally relate the temporal patterns to specific roads, and this condition may introduce memory context switching burden. Our method addresses both issues through in-place occlusion-free visualization of temporal patterns.

### 5.3 User Interactions

Apart from basic user interactions in map navigation and data selection, we support an additional of interactions to facilitate our analysis. Together with the temporal displays embedded into the roads, the interaction could largely enhances the capability of the system to address the tasks mentioned in Section 3.

**Brushing and Filtering** Users can directly brush any road segments on the map, which can be broadened by our route-zooming technique. Users can filter out data of interest by using the time interval in the time series curve, and the corresponding segments will be highlighted for all curves on the map. Locating a specific pattern of attributes in its occurring spatial and temporal positions could be well supported by this process.

**Overlaying** We support additional overlaying of optional labels, such as date time text labels, time axis, data value axis, traffic direction indicators, and user-specified texts.

**Road Width Control** To find the most appropriate width of a given road, users can select a road and then perform zooming to continuously enlarge or shrink the road. Together with overlaying, users could compare the temporal patterns embedded into the roads more effectively.

## 6 Experiments

We present two method instantiations to show the applicability of our route-zooming method. Then, we describe two case studies on real traffic flow data for demonstrating the usability of our spatio-temporal visualization.

### 6.1 Method Instantiations

In this section, we demonstrate two method instantiations of our route-zooming method including: (1) an interactive, focus+context metro map for city tourism and (2) illustrative maps for highlighting information on the broadened routes.

Many tourists usually prefer to travel by metro especially in a big city. However, large cities generally have fairly complex metro systems that are challenging for travel route planning and navigation. Our method can address this problem by overlaying key travel information on a broadened route in metro maps, which usually have special octilinear layouts, without significantly distorting the overall structure of the map. Figure 8(a) shows an interactive, focus+context map visualization for city tourism using a complex metro map in Tokyo, Japan. Whenever a tourist decides which attractions to visit in the city, we can determine a metro route that connects these attractions through various metro lines. The route can then be broadened by our route-zooming method. Each line segment of the broadened route keeps its original metro line color. The double circles encode important transfer stations. The attraction images are also overlaid on the broadened route at the corresponding metro stations. This example demonstrates that the technique is useful for city tourism. It enables tourists to interactively plan their travel route, such that he/she can see the key information (e.g., names of related metro lines and the major attractions) on the broadened route with the necessary context information and without any occlusion. It also allows tourists to easily travel in complex metro

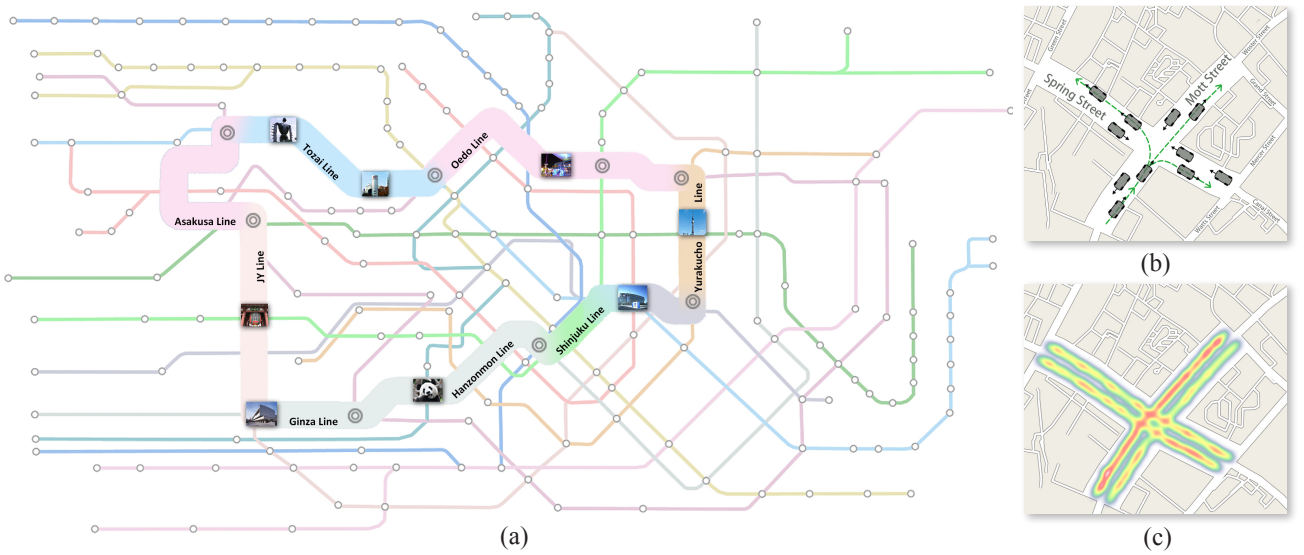


Fig. 8: Method instantiations of our route-zooming method for focus+context occlusion-free visualization: (a) a broadened tourist route with highlighted key information (e.g., images of tourist attractions and transfer stations highlighted); (b) a broadened road junction for a clear display of traffic simulation information; (c) a broadened road junction with a density map overlaid for visualization of two-way traffic flow information.

system because all key information (e.g., transfer stations) are highlighted clearly. It would be much more difficult for travel route planning and navigation in a complex metro system without our route-zooming technique.

Another method instantiation of our technique is for creating a static, illustrative map (e.g., poster) that can intuitively and clearly convey important information to wide audience. In this instantiation, user interactions are usually not allowed and important information should be displayed directly without occluding other context information. Figure 8 (b) shows that our technique can clearly illustrate a result of traffic simulation around a road junction. The method broadens the connecting roads and places the result on the roads without occluding or distorting context information. The broadened roads can even afford to display legible street names, which would be challenging without our technique. Our technique can further broaden the road to a larger extent with negligible distortion, so that additional information can be clearly displayed. Figure 8 (c) presents the same road junction with broader connecting roads to show a density map with two-way traffic flow information. Overlaying this density map with rich information on small, undeformed roads without using our technique can cause occlusion, while resizing the density map to fit small roads can result in illegible chart. Our result in Figure 8 (c) demonstrates that our technique creates a highly readable chart without the aforementioned problems.

The method instantiations discussed in this section demonstrate the applicability and usefulness of our technique in various applications.

## 6.2 Case Studies

In this section, we demonstrate the usefulness of our spatio-temporal visualization by conducting two case studies on real traffic flow data.

### 6.2.1 Data Preparation

We test our method using the taxi trajectory data that contains the trajectories of over 8000 taxis collected from November 1, 2011 to February 29, 2012, and from October 1, 2012 to October 31, 2013 in Hangzhou, China. The sampling rate is one sample every 20 seconds (on average), and the sampling duration is 24 hours each day. Each GPS record consists of seven fields: (*i*) ID; (*ii*) license number; (*iii*) latitude and longitude; (*iv*) status indicating whether the taxi is occupied or vacant; (*v*) date and time; (*vi*) direction; and (*vii*) speed. We calculate the number of taxis that passed by a road or a region of interest within each time period (e.g., one hour or one day), and then generate a time series curve representing the traffic flow of that road or region. We use this information in following analytical tasks.

### 6.2.2 Synoptic View of a Large Area

This case study demonstrates that our method can quickly identify interesting spatio-temporal patterns at the synoptic level. Figure 9 shows a synoptic view of the West Lake District in Hangzhou with two broadened roads. Each line chart on a broadened road segment encodes the taxi traffic flow of the road for one-week (from Monday to Sunday). Each repeated "wave" in a chart represents the traffic flow in one day. For example, Figure 9(a) represents the traffic flow on Tuesday. Each chart has two parts, namely, a green part and a red part. The green part represents the time series curve of traffic flow on right lanes (right side of the direction of the arrow), and the red part represents the left lanes (left side of the direction of the arrow). The synoptic view reveals the overall traffic conditions in the district and a user can further pursue interesting patterns spotted in the view (T1 and T3).

We find following interesting patterns in the synoptic view. A clear pattern of traffic imbalance is observed by comparing the green and red parts of the line charts (T3).

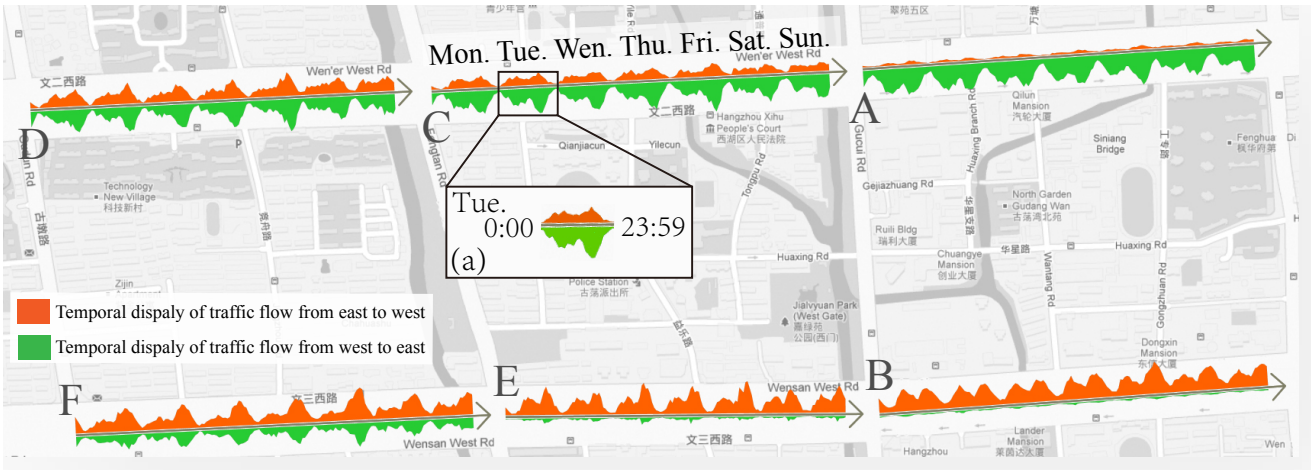


Fig. 9: A synoptic view of the traffic volume in the West Lake District allows quick detection of interesting patterns and easy comparison between multiple roads.

Roads A and B in the figure exhibit a high degree of traffic flow imbalance in two opposite directions. An investigation into the map reveals that roads A and B are both one-way roads. We also observe low degrees of traffic flow imbalance in roads C, D, E, and F, which are all two-way roads. The seamlessly integrated visualization embedding the temporal information into the map clearly shows us that roads C and D , and roads E and F are horizontally connected to roads A and B, respectively. The degree of traffic flow imbalance increases from west to east (i.e., from road D to C to A and from road F to E to B). Therefore, we surmise that the traffic flow imbalance in two-way roads C, D, E, and F are mainly due to the traffic flow imbalance of one-way roads A and B.

The temporal traffic flow patterns (see the line charts) are different for the two road types (T3). The patterns for the two-way roads (C, D, E and F) show that traffic during evening rush hours is heavier than that in the morning, which implies that the turnout rate of the taxis in the evening is higher than the one in the morning. In contrast, the patterns for one-way roads (A and B) indicate that traffic during morning rush hours is close to that in the evening. We surmise that since one-way roads afford higher traffic flow capacity over two-way roads, the taxi drivers typically enter the one-way roads whenever possible until the traffic becomes heavy in the morning and the evening.

This case study demonstrates the major benefit of our visualization that can assist analysts in quickly detecting and analyzing spatio-temporal patterns. If linked views are used to perform similar analysis tasks, then all of the time series must be examined and related to any discovered patterns on the map. This is inefficient and challenging because of the burden caused by context switching.

### 6.2.3 *Close Inspection of Local Regions*

In this case study, we demonstrate that our method allows users to quickly identify interesting spatio-temporal patterns through the examination and comparison of multiple temporal displays in different local regions of interest on the map (T1, T2, and T3). Figure 10 shows the broadened roads near railway station A and coach stations B, C, D, and E in Hangzhou. The temporal displays of taxi traffic flow near the stations are embedded into the roads. The rise and fall of the orange and blue time series curves represent the variations in taxi traffic flow for one week (from Monday to Sunday) in November 2011 and January 2013, respectively. The time granularity is set to one hour. The two curves are placed side by side in each display for a convenient comparison, and the arrow indicates the time direction (from Monday to Sunday).

The embedded view can quickly connect a temporal pattern of the corresponding station to its surrounding POIs (points of interest) (T2). Several noticeable patterns can be found in Figure 10. By comparing the taxi traffic flow for each station in two time periods, we can observe an imbalance of taxi traffic flow in several stations. At coach station B, the blue time series curve is much lower than the orange time series curve, which indicates that the taxi traffic flow significantly decreased from 2011 to 2013. This finding implies that fewer people chose to take a taxi to station B in 2013. With our in-place view, a quick examination of the POIs nearby revealed that there was also a station of Metro Line 1 at this coach station. We further found that the metro line started operating in November 2012. Since then, many people tended to ride the metro rather than take a taxis to station B. We surmise that it was because station B is far away from the downtown and people preferred to travel on the metro to save both time and money.

A different temporal pattern is observed at train station A (see Figure 10), which is also next to a Metro Line 1 station. The taxi traffic flow at this station (blue curve) increased in 2013 compared with the traffic flow (orange curve) in 2011. This may suggest that although more people chose to go to station A by metro after Metro Line 1 opened, the total number of people who traveled by train increased significantly since 2011. Therefore, the taxi traffic flow surrounding train station A still increased to a large degree. We speculate that this was caused by the accelerating development in high-speed rail in recent years,

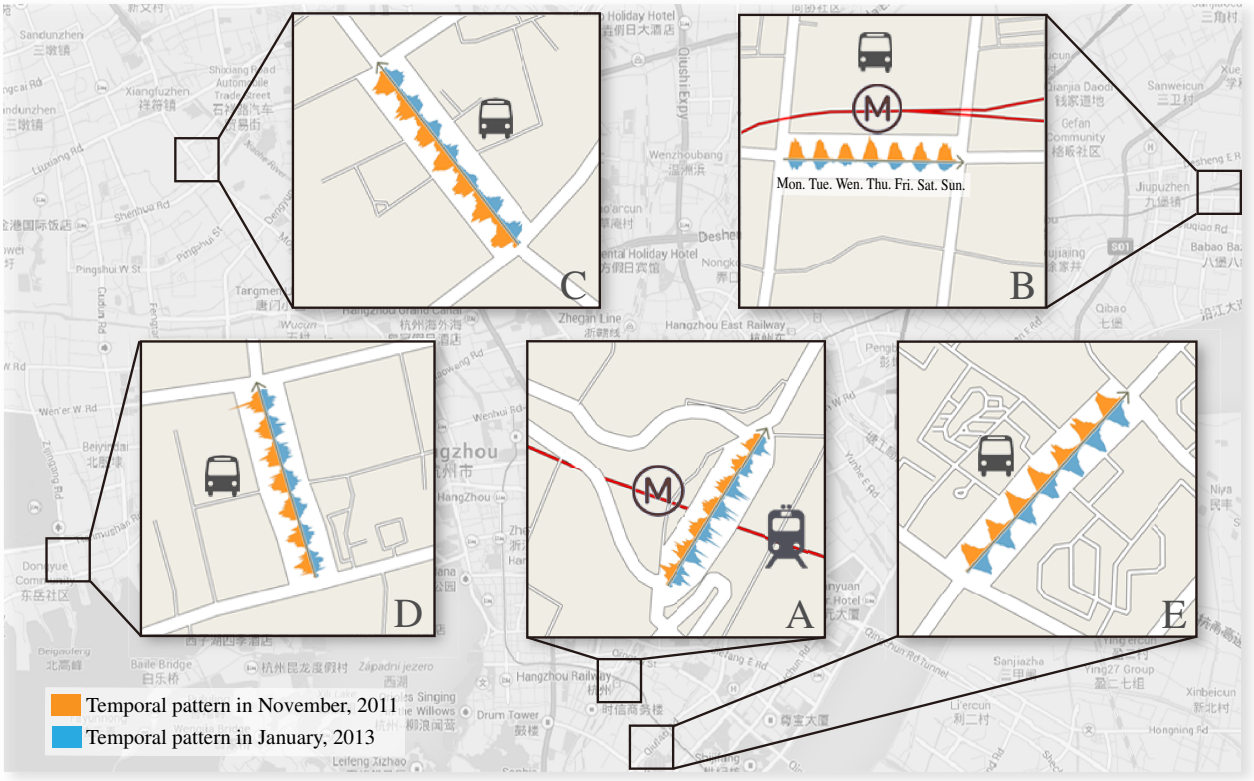


Fig. 10: Temporal pattern at one railway and four coach stations. The embedded view can help us quickly locate the temporal pattern with corresponding stations and surrounding points of interest.

which attracts more and more people to travel by train.

Moreover, we investigated the traffic flow imbalance of other coach stations, namely, stations C, D, and E. The blue curves (2013) are all lower than the orange curves (2011), which further proves that more passengers used the train whereas fewer passengers took a coach since 2011. However, the decrease in the taxi traffic flow of stations C, D, and E is not as significant as that of station B. A quick examination of the geographic locations of the three stations reveals that they are closer to the downtown than station B. Additionally, no metro station is found near the stations. Therefore, taking taxis to these stations was still popular for those who preferred to travel by coach.

The case study demonstrates that our embedded view is valuable and useful in integrating spatial and temporal information for efficient visual analysis. If a linked view or integrated view is used to explore these patterns, then switching between different views can occur or temporal displays could occlude the POIs.

## 7 User Studies

We evaluate the usability of our design based on a controlled user study. The user study is concerned with the performance of our method versus a linked view method.

### 7.1 Embedded View versus Linked View

A fare comparison of our method with other integrated views is difficult. First, obtaining the implementations of some methods is challenging. Second, the design goals are different. Our method aims to completely avoid occlusion that is undesirable for some applications. Thus, we compare our method with a standard linked view scheme (i.e., the map is in one window, while the time series curves are in another window), which also does not introduce occlusion.

Similar to the user study conducted by Dmitry et al. [18], we evaluate the effectiveness of our design with the linked view by running an experiment to address the following questions: *How do the embedded view or the linked view affect task completion time or accuracy? How does the orientation of roads in the embedded view or the linked view affect estimation time and accuracy?*

We hypothesize that the embedded view exhibits faster task completion than the linked view because the temporal information is directly associated with the corresponding spatial context. However, for the roads that are not horizontal, we expect longer response times for the embedded view due to the mental reorientation of temporal information. The error rate should be comparable in terms of accuracy.

**Method** In each trial, the subjects are provided a picture that shows three selected roads labeled Z, T, and R, respectively. The picture either contains three time series curves embedded in the three roads or displays three time series graphs on the right hand side of the map with clear labeling. The subjects are instructed to click on the road with the highest attribute value in a specified date as quickly as possible without compromising accuracy. The maps used in both methods have the same size. In other words, the bounding box that contains the linked view GUI is larger than that of the embedded view.

We test the embedded view and the linked view graphs with horizontal, vertical, or slanted roads in a within-subjects scheme. The trials are repeated five times for each condition. In generating the graphs for the experiment, we use the same map and dataset for both embedded view and linked view methods. The three roads in each trial have the same orientation. We control the practice effect by asking the subjects to practice as many times as they like for each graph type or road orientation until their performance became stabilized. The correct answers are provided for practice trials but not for test trials. We recruit 12 unpaid postgraduate students (6 male, 6 female) with engineering majors. Three of the subjects use time series curves frequently, two have seen time series curves from time to time, and the rest have rarely used them.

**Result and Discussion** Figure 11 presents the statistics for the study. Overall, the average response time is 3.03 seconds (SD = 0.84) for the embedded view and 4.37 seconds (SD = 1.11) for the linked view. We conducted a three Orientations (Horizontal, Vertical, Slanted) $\times$ two Techniques (Linked View, Embedded View) RM-ANOVA to analyze the response time data. Our analysis reveals a significant effect on the response time for both Techniques ($F(1,11) = 11.598$, $p < 0.01$) and Orientations ($F(2,22) = 4.531$, $p < 0.05$). However, a significant interaction for Techniques $\times$ Orientations is not observed. Pair-wise comparisons of Orientations show a significant difference between Horizontal roads and Slanted roads ($p < 0.01$); the other pairs do not have significant differences. The results confirm our hypothesis of the effects of different methods or orientations on response time. As for response accuracy, the overall average is 98.8% for the linked view and 99.4% for the embedded view.

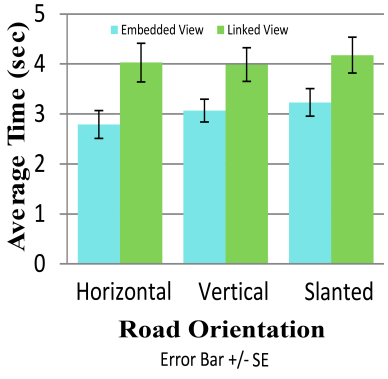


Fig. 11: Charts show the mean response time for the user studies with respect to *embedded view versus linked view.*

In addition, when the users finished the experiments, we asked the users to rate the performance when experiencing Embedded View or Linked View with respect to two questions: (Q1: can Embedded View help improve the performance of finding a specific traffic flow in different roads, or Q2: can Linked View help improve the performance of finding a specific traffic flow in different roads). Typical five-level Likert items are employed: Strongly agree (5), Agree (4), Neutral (3), Disagree (2), and Strongly disagree (1). Analysis of the results reveals that the average score of Q1 and Q2 are 4.83 (SD=0.38) and 2.18 (SD=0.87). Regarding Q1, all of the users report with Strongly Agree (10 users) or Agree (2 users); Regarding Q2, only one user report with Agree, and 66.7% users report with Strongly Disagree and Disagree.

### 7.2 Expert Evaluation

To evaluate the effectiveness of our design as well as the technique, we interviewed four domain experts (PA, PB, PC, and PD). PA is a leading researcher in urban-computing field, and has published papers at prestigious conferences and journals. PB is an associate professor in intelligent transportation field, and is active in solving problems facing traffic dispatching and controlling. PC and PD are from the bureau of transportation administration and an intelligent transportation company. They both have expertise in employing and developing real world transportation applications. However, except PA, the domain experts are not familiar with advanced visualization. During the interviews, we first gave a tutorial to introduce our work and the pipeline of route-zooming process for in-place visualization, and then demonstrate our real system to them to evaluate the effectiveness and usability of our technique. Their feedback is summarized as follows.

**Deformation and Cognitive Burden.** We showed the experts the process of broadening routes and embedding corresponding information (i.e., temporal displays for the city maps). The domain experts all agreed that the deformation to the map was acceptable. They found it difficult to notice the distortion to the whole map structure. PA said that "most of the sensible deformation occurs in certain context roads of the map", and "users most likely pay attention to the roads of interest (i.e., the broadening routes), and they may not notice the deformation to the context roads." This feedback is consistent with our aim of dispersing the deformation to the whole map structure to avoid obvious distortion. He further added that he appreciated our effort of ensuring the relative positions and angles among the roads, because it is essential for users to link the structure of original map and the deformed one. The domain experts all agreed that they did not experience additional cognitive burden or distraction when the road was broadened. PD mentioned that since many frequently used maps like tourist maps are also deformed or transformed to varying degrees for overlaying meaningful information, the deformation to the map appears not strange to her. However, PB found that the size of blocks between roads could be changed significantly during the road broadening in certain networks. We can address this issue by adding *virtual roads* (see Section 4.4) before roads are getting too close.

**Usability.** We presented the participants the two views for information presentation, namely, an embedded view where information is embedded into the broadened roads and a direct view where information is directly overlaid on routes for comparison. All of the domain experts confirmed the usefulness and effectiveness of the route-zooming approach, and they liked the embedded view for

information visualization due to its irreplaceable advantage, i.e., occlusion-free presentation. PB and PC both commented that the embedded view provides additional space for overlaying rich information while the direct view may hinder some critical information, for example, the exact intersection location between context roads and the road of interest. PB indicated that, for both drivers and transportation administrators, the embedded view would have the potential to play a critical role in certain circumstance such as crisis management and security monitoring.

**Suggestions** All of the domain experts provided valuable feedback on improving our work. PA, PB and PC all indicated that more applications should be explored using the route-zooming technique, for example, the navigation applications. PB suggested the technique should be able to be employed in navigation scenarios, such as navigating in reversible lanes or complex overpass bridges. PC also pointed out that "when users are driving to a destination using a navigation software, the technique has the advantage of allowing for overlaying various kinds of indication information such as real-time traffic accidents and ongoing road lane construction on the broadened road without occluding the navigation route". In addition, PD suggested that the technique should be able to support more kinds of maps such as hand-drawn cartoon maps.

## 8 Discussions

The experiments demonstrate that our graph-based route-zooming technique has clear advantages over other techniques. Compared with seam carving, our technique is more robust and efficient without distorting the context roads. Compared with linear zooming, our technique can highlight important information with faithful and rich spatial context. Our spatio-temporal visualization method based on route-zooming is also more useful and effective than other methods. Compared with linked views, our integrated visualization seamlessly embeds various information into meaningful spatial context and decreases the high cognitive overhead. Compared with integrated visualization based on simple information overlay, our method supports occlusion-free, focus+context visualization and is suitable for simultaneous comparative analysis of multiple roads.

However, our method still has some limitations. First, overlaying temporal displays on roads of unusual shapes may lead to a distortion problem. For example, if we need to embed a temporal display into a curved and irregular route, then we can reshape the display according to the route shape. However, the inner side of the display may be compressed, whereas the outer side may be stretched. To address this issue, we can introduce a constraint into our optimization process to ensure the consistency of the angle of incline for each road segment of the focus route. After the optimization, the curved route is not only broadened but also straightened such that the temporal display can be overlaid without any distortion. Nevertheless, straightening the focus route may also distort the geospatial context, which may mislead users in some circumstances. We plan to further study this problem balance the design trade-off.

Second, it is non-trivial to overlay temporal displays on roads of different lengths. If the temporal displays are simply stretched out to fit the roads, then they will have different size scales that can affect the subsequent comparative analysis. To address this issue, another constraint can be imposed to lengthen or shorten the roads in the optimization process. Specifically, for each road $e = \{u, v\}$, we can increase or decrease the distance between nodes $u$ and $v$. This constraint is particularly useful and effective when the road lengths are similar, because aligning a long road and a short road may lead to a noticeable distortion.

Finally, in some circumstances when a road having an abnormal shape does not allow an appropriate embedding of a temporal display, or when a great number of roads need to be broadened and the deformed map may exceed the screen resolution boundary, we can complement the visualization with other methods like traditional linked views.

## 9 Conclusion

In this work we present a novel technique called route-zooming to broaden a user selected focus route with the least distortion to the map. Based on the technique, we propose a new visualization solution that allows analysis and presentation of spatial and temporal data as an inseparable whole. Through the direct overlaying of time series visualizations on broadened roads, we achieve a seamless combination of space and time with no occlusion and minimal distortion. The usability of our system is demonstrated through two method instantiations and two case studies using real-world traffic data. The effectiveness and efficiency are proven by a user study compared with a conventional linked view design.

There are multiple possible avenues for future work. It would be useful to conduct a user centered experiment to evaluate the usability of different temporal visualizations embedded in the map. We also plan to conduct a systematic and quantitative evaluation on our route-zooming algorithm. One possible solution is to measure the difference between the deformed map and the original one by calculating the shifting distance of the each road in the two maps.

## Acknowledgment

The work is supported by National 973 Program of China (2015CB352503), NSFC (No. 61502416), Zhejiang Provincial NSFC (No. LR14F020002), joint project Data-Driven Intelligent Transportation between China and Europe announced by the Ministry of Science and Technology of China, and grant HK RGC GRF 618313.

## References

[1] W. Aigner, S. Miksch, H. Schumann, and C. Tominski. *Visualization of time-oriented data*. Springerverlag London Limited, 2011.

[2] G. Andrienko and N. Andrienko. Spatio-temporal aggregation for visual analysis of movements. In *Proceedings of the IEEE Symposium on Visual Analytics Science and Technology*, pages 51–58, 2008.

[3] G. Andrienko, N. Andrienko, U. Demsar, D. Dransch, J. Dykes, S. I. Fabrikant, M. Jern, M.-J. Kraak, H. Schumann, and C. Tominski. Space, time and visual analytics. *International Journal of Geographical Information Science*, 24(10):1577–1600, Oct. 2010.

[4] G. Andrienko, N. Andrienko, and M. Heurich. An event-based conceptual model for context-aware movement analysis. *International Journal of Geographical Information Science*, 25(9):1347–1370, Sept. 2011.

[5] S. Avidan and A. Shamir. Seam carving for content-aware image resizing. *ACM Transactions on Graphics*, 26(3):10:1–10:9, 2007.

[6] P. Bak, M. Schaefer, A. Stoffel, D. Keim, and I. Omer. Density equalizing distortion of large geographic point sets. *Cartographic and Geographic Information Science*, 36(3):237–250, 2009.

[7] T. Crnovrsanin, C. Muelder, C. D. Correa, and K.-L. Ma. Proximity-based visualization of movement trace data. In *Proceedings of the IEEE Symposium on Visual Analytics Science and Technology*, pages 11–18, 2009.

[8] H. Doraiswamy, N. Ferreira, T. Damoulas, J. Freire, and C. T. Silva. Using topological analysis to support event-guided exploration in urban data. *Visualization and Computer Graphics, IEEE Transactions on*, 20(12):2634–2643, 2014.

[9] G. W. Furnas. Generalized fisheye views. In *Proceedings of the SIGCHI Conference on Human Factors in Computing Systems*, pages 16–23, 1986.

[10] H. Guo, Z. Wang, B. Yu, H. Zhao, and X. Yuan. TripVista: triple perspective visual trajectory analytics and its application on microscopic traffic data at a road intersection. In *Proceedings of the IEEE Pacific Visualization Symposium*, pages 163–170, 2011.

[11] J.-H. Haunert and L. Sering. Drawing road networks with focus regions. *IEEE Transactions on Visualization and Computer Graphics*, 17(12):2555–2562, Dec. 2011.

[12] Y. Ivanov, C. Wren, A. Sorokin, and I. Kaur. Visualizing the history of living spaces. *IEEE Transactions on Visualization and Computer Graphics*, 13(6):1153–1160, Nov. 2007.

[13] T. Kapler and W. Wright. Geotime information visualization. In *Proceedings of the IEEE Symposium on Information Visualization*, pages 25–32, 2004.

[14] R. Kincaid. SignalLens: focus+context applied to electronic time series. *IEEE Transactions on Visualization and Computer Graphics*, 16(6):900–907, Nov. 2010.

[15] H. Liu, Y. Gao, L. Lu, S. Liu, H. Qu, and L. Ni. Visual analysis of route diversity. In *Proceedings of the IEEE Symposium on Visual Analytics Science and Technology*, pages 171–180, Oct. 2011.

[16] P. McLachlan, T. Munzner, E. Koutsofios, and S. North. LiveRAC: interactive visual exploration of system management time-series data. In *Proceedings of the SIGCHI conference on Human factors in computing systems*, pages 1483–1492. ACM, 2008.

[17] T. Munzner, F. Guimbretière, S. Tasiran, L. Zhang, and Y. Zhou. TreeJuxtaposer: scalable tree comparison using focus+ context with guaranteed visibility. *ACM Transactions on Graphics*, 22(3):453–462, 2003.

[18] D. Nekrasovski, A. Bodnar, J. McGrenere, F. Guimbretière, and T. Munzner. An evaluation of pan & zoom and rubber sheet navigation with and without an overview. In *Proceedings of the SIGCHI conference on Human Factors in computing systems*, pages 11–20. ACM, 2006.

[19] E. Pietriga, O. Bau, and C. Appert. Representation-independent in-place magnification with sigma lenses. *IEEE Transactions on Visualization and Computer Graphics*, 16(3):455–467, May 2010.

[20] H. Qu, H. Wang, W. Cui, Y. Wu, and M.-Y. Chan. Focus+context route zooming and information overlay in 3d urban environments. *IEEE Transactions on Visualization and Computer Graphics*, 15(6):1547–1554, Nov. 2009.

[21] R. Scheepens, N. Willems, H. van de Wetering, and J. J. van Wijk. Interactive visualization of multivariate trajectory data with density maps. In *Proceedings of the IEEE Pacific Visualization Symposium*, pages 147–154, 2011.

[22] G. Sun, Y. Liu, W. Wu, R. Liang, and H. Qu. Embedding temporal display into maps for occlusion-free visualization of spatio-temporal data. In *Proceedings of the IEEE Pacific Visualization Symposium*, pages 185–192, 2014.

[23] C. Tominski, S. Gladisch, U. Kister, R. Dachselt, and H. Schumann. A Survey on Interactive Lenses in Visualization. In *Proceedings of EuroVis State-of-the-Art Reports*, pages 43–62, 2014.

[24] C. Tominski, H. Schumann, G. Andrienko, and N. Andrienko. Stacking-based visualization of trajectory attribute data. *IEEE Transactions on Visualization and Computer Graphics*, 18(12):2565–2574, Dec. 2012.

[25] T. C. van Dijk and J.-H. Haunert. Interactive focus maps using least-squares optimization. *International Journal of Geographical Information Science*, 28(10):2052–2075, 2014.

[26] Y.-S. Wang and W.-Y. Peng. Interactive metro map editing. *IEEE Transactions on Visualization and Computer Graphics*, 22(2):1115–1126, Feb. 2016.

[27] Z. Wang, T. Ye, M. Lu, X. Yuan, H. Qu, J. Yuan, and Q. Wu. Visual exploration of sparse traffic trajectory data. *Visualization and Computer Graphics, IEEE Transactions on*, 20(12):1813–1822, 2014.

[28] M. Q. Wang Baldonado, A. Woodruff, and A. Kuchinsky. Guidelines for using multiple views in information visualization. In *Proceedings of the Working Conference on Advanced Visual Interfaces*, pages 110–119, 2000.

[29] J. Yuan, Y. Zheng, X. Xie, and G. Sun. T-drive: Enhancing driving directions with taxi drivers' intelligence. *IEEE Transactions on Knowledge and Data Engineering*, 25(1):220–232, 2013.

[30] J. Zhao, F. Chevalier, E. Pietriga, and R. Balakrishnan. Exploratory analysis of time-series with chronolenses. *IEEE Transactions on Visualization and Computer Graphics*, 17(12):2422–2431, Dec. 2011.

**Guodao Sun** is an assistant professor at the College of Information Engineering, Zhejiang University of Technology, Hangzhou, China. He received the B.Sc. in computer science and technology, and Ph.D. degree in control science and engineering both from Zhejiang University of Technology. His main research interests are urban visualization and visual analytics of social media.

**Ronghua Liang** received the Ph.D. in computer science from Zhejiang University in 2003. He worked as a research fellow at the University of Bedfordshire, UK, from April 2004 to July 2005 and as a visiting scholar at the University of California, Davis, US, from March 2010 to March 2011. He is currently a Professor of Computer Science and Dean of College of Information Engineering, Zhejiang University of Technology, China. He has published more than 50 papers in leading international journals and conferences including IEEE TKDE, IEEE TVCG, IEEE VIS, IJCAI, AAAI. His research interests include Visual Analytics, Computer Vision, and Medical Visualization.

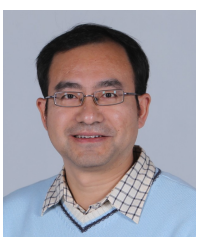

**Huamin Qu** is a professor in the Department of Computer Science and Engineering (CSE) at the Hong Kong University of Science and Technology. His main research interests are in visualization and human-computer interaction, with focuses on urban informatics, social network analysis, e-learning, and text visualization. He obtained a BS in Mathematics from Xi'an Jiaotong University, China, an MS and a PhD in Computer Science from the Stony Brook University.

**Yingcai Wu** is an assistant professor at the State Key Lab of CAD CG, Zhejiang University, Hangzhou, China. He received his Ph.D. degree in Computer Science from the Hong Kong University of Science and Technology (HKUST). Prior to his current position, Yingcai Wu was a researcher at the Internet Graphics Group in Microsoft Research Asia, Beijing, China. His primary research interests lie in visual behavior analytics, visual analytics of social media, visual text analytics, uncertainty-aware visual analytics, and information visualization. For more information, please visit http://www.ycwu.org.